Adipose tissue mitochondrial respiration in Atlantic salmon: implications for sex-dependent life-history variation

Jenni M. Prokkola*[§1,6], Anita Wagner*[2,5], Elisabeth Koskinen[1], Paul V. Debes[1,3], Andrew House[1], Eirik R. Åsheim[1,4], Craig R. Primmer[1,4], Eija Pirinen[2,5], Tutku Aykanat[1]

[1] Organismal and Evolutionary Biology Research Programme, Faculty of Biological and Environmental Sciences, University of Helsinki, Helsinki, Finland

[2] Research Program for Clinical and Molecular Metabolism, Faculty of Medicine, University of Helsinki, Helsinki, Finland

[3] Department of Aquaculture and Fish Biology, Hólar University, Sauðárkrókur, Iceland

[4] Institute of Biotechnology, Helsinki Institute of Life Science (HiLIFE), University of Helsinki, Helsinki, Finland

[5] Research Unit for Internal Medicine, Faculty of Medicine, University of Oulu, Oulu, Finland

[6] Natural Resources Institute Finland (LUKE), Oulu, Finland

* Equal contribution

[§] Corresponding author, jenni.prokkola@luke.fi, +358 29 532 2614, Natural Resources Institute Finland (LUKE), Paavo Havaksen tie 3, FI-90014 Oulun yliopisto, Oulu, Finland

Short title: Adipose tissue mitochondrial respiration in salmon

Keywords: metabolism, sexual maturation, puberty, white adipose tissue

Author contributions:

Conceptualization: JMP, AW, PVD, CRP, EP, TA

Formal analysis: JMP, AW, EP, TA

Funding acquisition: CRP, EP, TA

Investigation: JMP, AW, EK, PVD, AH, ERÅ, CRP, EP, TA

Methodology: JMP, AW, EK, EP, TA

Resources: PVD, AH, ERÅ, CRP, EP, TA

Supervision: EP, TA, CRP

Visualisation: JMP, AW, EP, TA

Writing – Original Draft Preparation: JMP, AW, EP, TA

Writing – Review & Editing: JMP, AW, EK, PVD, AH, ERÅ, CRP, EP, TA

Abstract

Adipose tissue is essential for energy homeostasis, with mitochondria having a central role in its function. Mitochondria-mediated adipose tissue dysfunction has been linked to several metabolic disorders in humans but surprisingly little is known about whether variation in adipose tissue processes, such as mitochondrial function, is maintained in wild animal populations, how it is related to reproductive success, and its evolutionary significance. Early sexual maturation (age-at-maturity) in Atlantic salmon (*Salmo salar*) is promoted by higher adiposity and has a strong genetic association with the *vestigial like 3* (*vgll3*) locus. Vgll3 is also linked to the control of adipose tissue growth and pubertal timing in mammals. This makes Atlantic salmon ideal for studying whether functional variation in adipose tissue processes is linked to reproductive timing. Here, using 16 Atlantic salmon individuals of different sexes reared in common-garden conditions, we conducted a proof-of-principle study and tested whether mitochondrial respiration in adipose tissue, mitochondrial DNA (mtDNA) amount, and adipocyte size are associated with sex and *vgll3* genotype. Mitochondrial respiration was quantified from freshly collected white adipose tissue using high-resolution respirometry, and mtDNA amounts were quantified relative to nuclear DNA amounts. We found differences in mtDNA amount between sexes, plausibly caused by a confounding effect of maturation status, but without corresponding differences in mitochondrial respiration. Mitochondrial respiration, leak respiration, and coupling capacity (P/E ratio) were marginally lower in immature females carrying the *vgll3* early maturation genotype compared to those with the late maturation genotype, although larger sample sizes are required to validate this difference. Our results generate new hypotheses on how coupling capacity of oxidative phosphorylation could be linked with the timing of maturation via adiposity as well as pave the way to study the mechanistic relationships between life-history variation and mitochondrial bioenergetics in wild populations.

Introduction

Energy allocation dynamics are central to theories of life-history evolution. At the theoretical level and in ecological studies, adipose tissue, which is the major energy storage organ in animals, is often viewed as an “inert” energy storage. In reality, adipose tissue affects normal metabolic functions and reproductive fitness in animals in multiple ways (1). White adipose tissue is the most abundant type of adipose tissue, localising mainly to subcutaneous and visceral depots. The main function of white adipose tissue is to store the dietary energy in the form of fat (triglycerides) and allocate energy to other tissues by mobilizing stored fat during fasting and high energy demand processes such as growth and sexual maturation (1). The endocrine function of adipose tissue, *i.e*., secretion of hormones and bioactive molecules, also controls whole-body energy homeostasis and facilitates the communication between adipose tissue and other organs (2). The key functions of adipose tissue are dependent on mitochondria –the organelles that produce metabolites and energy for cells (3-6)– yet how adipose tissue mitochondrial function is linked to life-history traits and fitness is poorly understood.

Mitochondria are dynamic organelles – their number and efficiency to produce adenosine triphosphate (ATP) are affected by the energetic status of the cell, which depends on environmental conditions and tissue type, among other factors (7, 8). Mitochondrial function can be assessed by quantifying mitochondrial respiration via oxidative phosphorylation (OXPHOS), a cascade of reactions taking place across the inner mitochondrial membrane. In OXPHOS, electrons from NADH and FADH2 are transferred through a chain of protein complexes, namely complexes I-IV, ubiquinone (Q) and cytochrome c, and finally to the electron acceptor oxygen (Fig. 1a). Simultaneously, complexes I, III, and IV pump protons into the mitochondrial intermembrane space, generating a proton gradient that drives the phosphorylation of ADP to ATP by the ATP synthase enzyme. The efficiency of mitochondrial respiration is determined by the proportion of electrons in OXPHOS that are coupled to generating ATP (coupled respiration), *versus* proton leakage and electron slippage across the inner membrane (uncoupled respiration) (Fig 1a). Intact tissues exhibit both coupled and uncoupled OXPHOS, whereby highly efficient mitochondria are tightly coupled (9).

Energy metabolism is central to diversity within species; variation in the organisation and efficiency of mitochondria among individuals is likely under selection and adaptive (10, 11). Within species, how variation in mitochondrial function could lead to variation in other traits can

be better understood by measuring the different stages and efficiency of mitochondrial respiration (see e.g., (10). For example, the ability to increase ATP synthesis, which requires sufficient reserve capacity in the electron transport pathway, allows organisms to respond *via* mitochondria to changes in energetic demand and environmental stressors (12, 13). Likewise, although proton leak reduces the efficiency of mitochondria, it may restrict the production of reactive oxygen species and may thereby limit oxidative stress (14). Variation in mitochondrial processes may thus allow individuals to respond differently to energetic demand and stressors. Despite the central role of mitochondria in the control of adipose tissue function, little is known of how adipose tissue mitochondrial activity relates to growth and body condition and affects life-history traits, such as the timing of sexual maturation (15). The fact that obesity in humans is associated with a significant decline in adipose tissue mitochondrial respiration (6, 16) also makes it appealing to study adipose tissue mitochondria in relation to life-history decisions in other species.

Critical time points of an organism's life cycle constitute life-history traits, the variation in which is largely shaped by energy allocation differences and maintained within species via evolutionary trade-offs (17). In Atlantic salmon (*Salmo salar*), earlier maturation shortens generation time and increases the survival probability prior to reproduction compared to delayed maturation, but this comes at the expense of smaller size at maturity, which is associated with lower fecundity (18). The Atlantic salmon is an emerging wild model species to study the energetic basis of life-history adaptations for two main reasons (15, 19). First, faster accumulation of adipose tissue, quantified as a high condition factor, is closely related to earlier sexual maturation in salmon, and higher fat content has been found in juvenile males compared to females before male early maturation occurs (20-22). Second, a single genomic region explains a substantial amount of variation in age-at-maturity (23). The strongest candidate gene in this region, *vgll3* (24), is likely important for adipose tissue growth and function; in mice, expression of *vgll3* was negatively correlated with adipose tissue mass and body weight (25), and in humans, variation in the *VGLL3* locus is associated with the timing of puberty (26, 27). Finally, *vgll3* early maturation genotype is linked to higher body condition in salmon (20). Therefore, adipose tissue processes could provide a functional basis of variation in age-at-maturity, and subsequently, potential evolutionary constraints (15, 19).

In this study, we first measure mitochondrial quantity and respiration as well as adipocyte morphology in the visceral adipose tissue of Atlantic salmon – as fishes are not known to have

brown adipose tissue, the focus is on white adipose tissue (28). We then investigate sex- and *vgll3* genotype -dependent differences in mitochondrial respiration to obtain preliminary insights into whether mitochondrial function is a potential cellular pathway underlying life-history variation in salmon.

Material and Methods

Fish rearing and sampling

The experiment was approved by the Finnish Animal Experiment Board (ESAVI/42575/2019). Samples of adipose tissue were collected from fish reared as part of another study during August-September 2020 and were approximately 2 years 8 months post hatch (average mass 1kg (Table 2)). Details of fish rearing, feeding, and temperatures are shown in (29) until Feb 2020 (in Feb-Aug 2020, conditions largely followed those in 2019). We collected samples from Neva population individuals from the high temperature treatment. The mean (±SD) temperature during the sampling period was 11.7 ± 0.8°C.

The fish were fasted for ~57 hours prior to sampling. One day prior to sampling, the individuals, which had been previously tagged with passive integrated transponders (PIT-tags) and identified for *vgll3* genotype and sex, were selected for sampling, anaesthetised with buffered tricaine methanosulfonate (MS-222, 0.125g/L, sodium bicarbonate buffered), and measured for body mass (to the nearest 0.1g) and fork length (to the nearest mm). After measurement, the fish were placed in a floating cage held inside the rearing tank until sampling the following day. The sampling was balanced in terms of sex and *vgll3* genotypes across four sampling days (from in total four tanks), on which four individuals (one female and one male of both EE and LL genotypes, referring to homozygous early and late maturation genotypes, respectively) from within the same rearing tank were captured by netting each day and euthanized with an overdose of MS-222 (0.250g/L, sodium bicarbonate buffered). Fish were sampled from a different rearing tank between 8:40 and 11:40 AM on each day of sampling; three tanks had been reared with normal feed used in Atlantic salmon aquaculture (control), and one tank with a low-fat feed diet (details in (29)). Visceral adipose tissue samples were collected using sterilized equipment within ~30 min of euthanasia and 1) stored in BIOPS (2.77 mM CaK_2EGTA, 7.23 mM K_2EGTA, 20 mM imidazole, 20 mM taurine, 50 mM MES hydrate, 0.5 mM DTT, 6.56 mM $MgCl_2$, 5.77 mM ATP and 15 mM phosphocreatine (30)), or 2) flash-frozen in liquid nitrogen and stored

at -80°C. Samples in BIOPS were kept on ice and transported to Meilahti campus, University of Helsinki, for mitochondrial respiration measurements (see schematic illustrations Fig. 1b-c). After sample collection, all following analyses were performed blind with respect to the diet treatment, genotype, and sex of fish.

The maturation status of the fish was determined from the appearance of gonads. All males had partially enlarged gonads indicating that the maturation process had started (the gonads of most of the remaining males in the experimental population were fully matured roughly two months after the sampling [E. Å., personal observation]), and all females had immature gonads, i.e., small eggs that covered only a small part of the body cavity, except one female that showed more advanced maturation indicated by gonad mass that was on average 30 times larger than in the other females. The mature female was excluded from the analyses.

High-resolution respirometry

Visceral adipose tissue stored in BIOPS buffer was used in high-resolution respiration measurements with Oxygraph-2k equipment (O2k, Oroboros Instruments, Innsbruck, Austria) (Fig.1d). Adipose tissue was dried by blotting on a tissue paper and weighed before placing it into a calibrated chamber with the Mir05 buffer (0.5 mM EGTA, 3 mM $MgCl_2$, 60 mM lactobionic acid, 20 mM taurine, 10 mM KH_2PO_4, 20 mM HEPES, 110 mM D-sucrose, 1 g/L BSA), (30)) (Fig 1c). We used 28–50mg adipose tissue in each measurement (Tables 2 and S2). The measurements were performed at 12°C under constant stirring (750rpm) and oxygen concentration was kept above 250µM. Oxygen flux was calculated as means over ~1 min within each measured parameter after a stable flux was achieved.

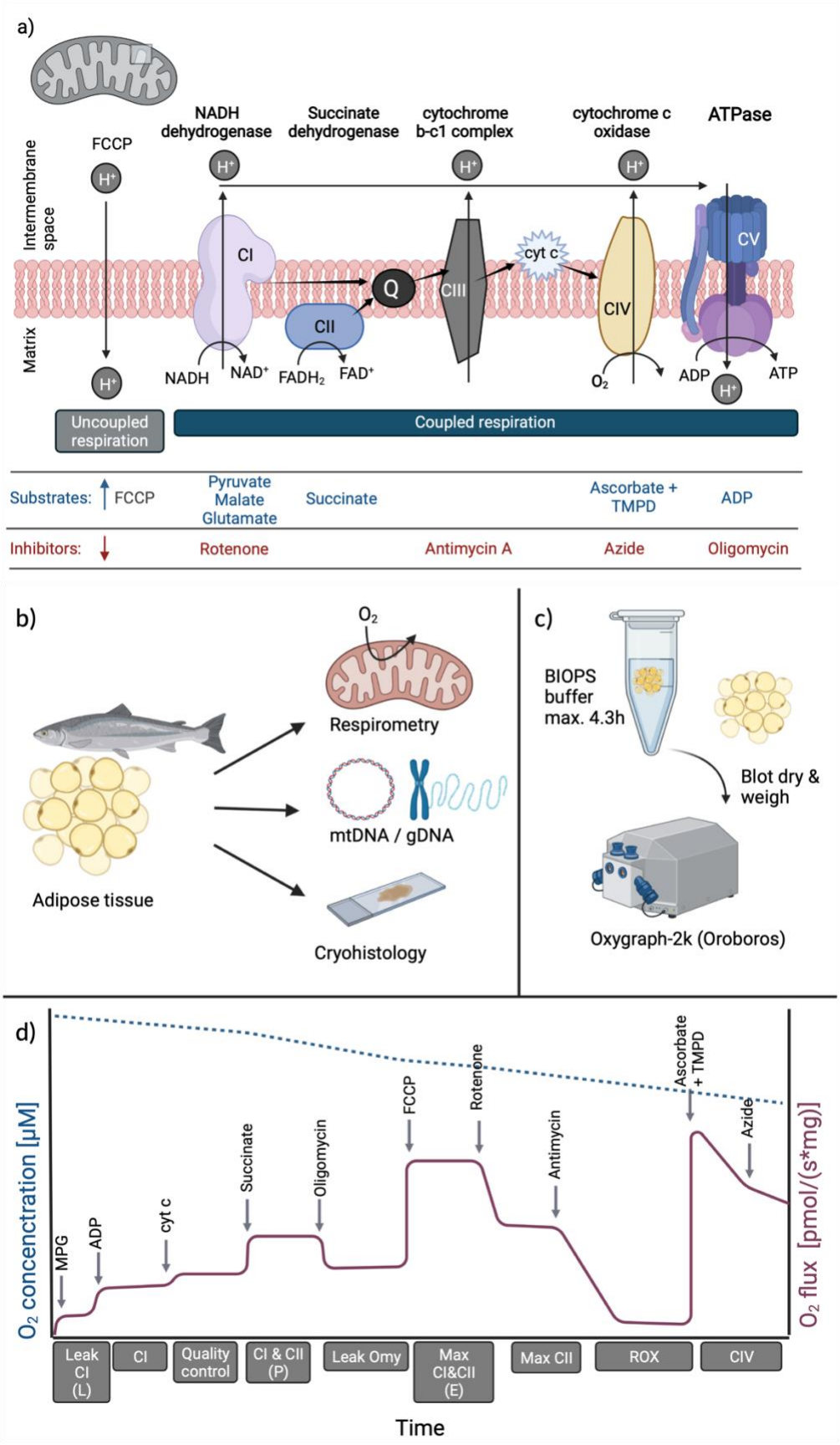
a)
NADH dehydrogenase
Succinate dehydrogenase
cytochrome b-c1 complex
cytochrome c oxidase
ATPase
FCCP
Intermembrane space
Matrix
CI
CII
CIII
CIV
CV
Q
cyt c
NADH
NAD+
FADH2
FAD+
O2
ADP
ATP
Uncoupled respiration
Coupled respiration
Substrates:
FCCP
Pyruvate
Malate
Glutamate
Succinate
Ascorbate + TMPD
ADP
Inhibitors:
Rotenone
Antimycin A
Azide
Oligomycin
b)
Adipose tissue
Respirometry
mtDNA / gDNA
Cryohistology
c)
BIOPS buffer max. 4.3h
Blot dry & weigh
Oxygraph-2k (Oroboros)
d)
O2 concentration [µM]
O2 flux [pmol/(s*mg)]
MPG
ADP
cyt c
Succinate
Oligomycin
FCCP
Rotenone
Antimycin
Ascorbate + TMPD
Azide
Leak CI (L)
CI
Quality control
CI & CII (P)
Leak Omy
Max CI&CII (E)
Max CII
ROX
CIV
Time

184

Fig. 1. A schematic illustration of oxidative phosphorylation (OXPHOS), the study design, and the substrate-uncoupler-inhibitor respirometry protocol. (a) OXPHOS and the relevant respiration substrates and inhibitors used in this study. Electrons are shown as tapered black arrows. (b-c) The methodologies applied for visceral adipose tissue samples. (d) The injection protocol used in high-resolution respirometry with the Oxygraph 2k, with a schematic oxygen flux curve in purple. The calculated respiration parameters are shown below the x-axis (d). MPG = malate, pyruvate, glutamate. ROX = residual oxygen flux. Figures created with BioRender.

Substrate-uncoupler-inhibitor respirometry protocol (Fig. 1d) was used to determine LEAK (dissipative, non-OXPHOS respiration), OXPHOS (respiration coupled to phosphorylation of ADP to ATP) and ETS (electron transfer system uncoupled from the phosphorylation) respiration states. The stock solutions and final concentrations of substrates, uncoupler, and inhibitors used are presented in Table 1. To determine CI - mediated leak respiration, the NADH-pathway substrates malate, pyruvate and glutamate were added. After a stable plateau was formed, ADP at the saturating concentration was premixed with MgCl and added to induce coupled phosphorylating CI (NADH)-linked respiration. Mitochondrial outer membrane integrity was evaluated by the lack of response to the addition of cytochrome c. Next, to measure CI & CII -mediated respiration, succinate was injected to induce the electron flow through CII. After O_2 flux was stabilised, the ATP synthase inhibitor, oligomycin, was added to determine CI&CII mediated leak respiration. To measure the maximal ETS capacity of CI&CII-linked respiration, the stepwise addition of the uncoupler carbonyl cyanide-p-trifluoromethoxyphenylhydrazone (FCCP) was performed. This was followed by inhibition of CI with rotenone to determine the maximal ETS capacity via CII. After blocking electron transfer with antimycin, the complex III inhibitor, residual oxygen flux (ROX) was quantified. Complex IV (CIV) activity was determined by adding N,N,N',N'-Tetramethyl-p-phenylenediamine dihydrochloride (TMPD) as a substrate in conjunction with the reducing agent ascorbate. Complex IV was inhibited with sodium azide to correct previous results for the chemical auto-oxidation of reagents (31). Oxygen flux was quantified using the DatLab analysis software (30). ROX was subtracted from all except CIV-related values. The delay until the respiration measurements started after the fish were euthanized ranged from 1.8 to 4.3 hrs, but this was not correlated with oxygen flux during the measurements (Fig. S1).

Table 1. The used reagent concentrations and their respective respiration parameters and states.

Reagent	Site of action	Stock solution	Final concentration	Parameter	Respiration state
Malate /l-malic acid (M) Pyruvate/Pyruvic acid (P) Glutamate/l-Glutamic acid (G)	Complex I substrate	400mM 2M 2M	2mM 10mM 10mM	Leak CI (L)	LEAK
Adenosine diphosphate (ADP) Magnesium chloride (MgCl)	ATP synthase substrate	500mM 300mM	5mM 2.5mM	CI	OXPHOS
Cytochrome c (Cyt c)	Test of outer membrane integrity	4mM	10µM	Quality control	
Succinate (Suc)	Complex II substrate	1M	10mM	CI&CII (P)	OXPHOS
Oligomycin (Omy)	Inhibitor of ATP synthase	5mM	2.5µM	Leak Omy	LEAK
Carbonyl cyanide-p-trifluoromethoxy-phenylhydrazone (FCCP)	Uncoupler of ETS	1mM	Titration in 0.5µM to 1.2µM (1-3µL) steps. Final concentration 18µM	Max CI&CII (E)	ETS
Rotenone (R)	Inhibitor of CI	1mM	0.5µM	Max CII	ETS
Antimycin A (Ama)	Inhibitor of CIII	5mM	2.5µM	Residual oxygen flux (ROX)	
Tetramethylphenylendiamin (TMPD)	CIV substrate	200mM	0.5mM	CIV	ETS
Ascorbate (Asc)	Reducing agent for TMPD	800mM	2mM	CIV	ETS
Azide (Az)	Inhibitor of CIV	4M	20mM	CIV	ETS

We calculated mitochondrial respiration coefficients from tissue mass -normalised parameters shown in Table 1 and Fig. 1d as follows: *NADH pathway cofactor (NADH)*: CI / CI&CII, indicating the proportion of CI respiration from CI & CII respiration; *Succinate pathway cofactor*

(Succ): 1 - CI / CI&CII, indicating the proportion of CII respiration from CI & CII respiration; *Coupling efficiency (CoupEff)*: (CI&CII - Leak Omy) / CI&CII, indicating the proportion of ATP synthesis -linked respiration from CI & CII respiration; *Coupling control ratio (L/P):* Leak CI / CI&CII, indicating the proportion of CI-linked proton leak from CI & CII respiration; and *Coupling capacity (P/E)*: CI&CII / max CI&CII, indicating the proportion of phosphorylating, coupled CI & CII mediated respiration from non-phosphorylating, uncoupled CI & CII mediated respiration.

Measurements of mitochondrial DNA content

We quantified mtDNA amount relative to nuclear genomic DNA (gDNA) as a proxy for mitochondrial content per cell (32) to understand whether mitochondrial respiration variation was explained by differences in mitochondrial number or function. The tissue used in this procedure was collected at the same time as the sample used in the high-resolution respiration measurements. First, DNA was extracted using a slightly modified conventional phenol-chloroform extraction. Phenol chloroform extraction conserves different sizes of DNA relatively similarly compared to silica column-based extraction protocols, hence exhibiting higher reproducibility when quantifying mtDNA to gDNA ratio (33). Briefly, approximately 100 mg of adipose tissue and a 7 mm metal bead were placed in a 2 mL centrifuge tube containing 0.5 ml PBS buffer (pH 7.4) and homogenised in TissueLyser II (Qiagen) for 2 minutes at 25 Hz. The homogenate was then incubated overnight at 37°C in 0.6 ml lysis buffer (10 mM Tris–HCl, 1 mM EDTA, and 0.1% SDS, pH 8.0) with 7 µL proteinase K solution (20mg/mL), and then treated with RNAase (0.2 mg/mL) for 30 min at 37°C. Next the solution was treated with 600 µL phenol (VWR, Tris-buffered, pH=6.6) twice, followed by two 500 µL chloroform isoamyl alcohol (24:1) washes. A 1:10 volume of sodium acetate (3M, pH 5.2) and 2.5 volumes of ice-cold ethanol was then added to the aqueous phase and samples were incubated for 30 min at -20°C. The precipitated DNA was then washed twice with 70% ethanol, air dried for 30 min, and resuspended in 50 µL TE solution (5 mM Tris, 0.1 mM EDTA, pH 8.0) for 15 min at 37°C. DNA quality and quantity were assessed using Nanodrop 2000 (Thermo Scientific) and DNA concentration was adjusted to 5 ng/µL. All samples in the analyses had 260/280 ratios greater than 1.80 (average = 1.90, SD = 0.05), indicating high purity. DNA was extracted in two batches for n = 12, and n = 8 samples, respectively, where four samples were extracted twice to control for batch effects (totalling16 samples); these samples were run in six replicate reactions, while the others were run in triplicates.

Next, quantitative real-time PCR (qPCR) was performed using a double-stranded DNA-binding dye as a reporter (HOT FIREPol EvaGreen qPCR Supermix, Solis Biodyne), in a 384-plate format using a Biorad CFX384 C1000 thermal cycler. We targeted two mitochondrial (*16s* and *cytb)*, and two nuclear (*app*, *EF1a*) genomic regions using a double-stranded DNA-binding dye (eva green) as a reporter. Primers specific to these genomic regions were designed with Primer-BLAST (34), where the melting temperature (Tm) and product size were adjusted to 59–61°C, and 90–150 bp, respectively (Table S1).

The qPCRs were run for 45 cycles at 95°C, 58°C, and 72°C for 15, 20, and 20 s, respectively, following initial denaturation at 95°C for 12 min. The volume of reactions was 10 µL, with 2 µL 5x HOT FIREPol EvaGreen qPCR Supermix (Solis Biodyne, Tartu, Estonia), 150 nM of each primer, and 5 µL diluted DNA (total 1.67 ng). Samples were analysed in triplicates for each marker.

The relative mtDNA to gDNA amount, where gDNA amount was first divided by two to account for two copies of gDNA per cell, was then quantified from mean expression across replicate reactions using an efficiency-corrected method (35). Ct values and PCR efficiencies were calculated using LinregPCR (36), where baseline correction and window-of-linearity analysis (the cycles with the highest linear correlation) was performed separately for each well and the efficiency of each primer set was calculated as the mean of individual wells' efficiency.

Measurements of adipocyte size

Flash-frozen samples of visceral adipose tissue were sectioned to assess whether adipocyte size correlated with mitochondrial respiration. Samples were embedded in the Optimal Cutting Temperature compound and sectioned to 20-30 µm at -50°C using a cryostat (Leica CM 3050S) and stained with haematoxylin & eosin using Sakuras Tissue-Tek DRS 2000 at the Department of Anatomy, University of Helsinki following a standard protocol. In brief, cryosections were fixed with ice-cold acetone for 10 min on ice, air dried for 30 min, washed twice with PBS for 1 min, incubated in PBS for 10 min, washed in water for 1 min, stained with Mayer's hemalum solution (Merck) for 5 min, washed with tap water for 1 min, incubated in distilled water for 1 min, stained with May-grunwald's eosin-methylene blue solution modified (Merck) for 3 min, and washed in tap water for 1 min, and twice each in 96% ethanol for 20 s, Abs ethanol 5 min, and Xylene 2 min. Finally, slides were covered with Pertex mounting medium (Histolab).

The slides were imaged using 20x magnification with extended plane, using 3DHISTECH Pannoramic 250 FLASH II digital slide scanner. Images were inspected in Qupath v. 0.3.0 (37) and 1–2 regions containing visceral adipose tissue from each image were saved in tiff format. Tiff-images were analysed in ImageJ to measure the size of particles with a size of 1000–100000 and circularity of 0.2–1.00 as size and shape filters (used macro in Appendix S2). The selected cells were visually inspected to exclude selections that were merged of multiple cells, were stretched (during sectioning) or had a very irregular shape because of excess dye. The remaining selected cells were measured (area in μm^2) (see Fig. 2a for a representative image). The number of cells identified with this method ranged from 40 to 306 between individuals due to the variable size and quality of the sections. However, the number of measured cells was not correlated with mean (Spearman-rho = -0.24, p = 0.426) or median (Spearman-rho = -0.26, p = 0.388) adipocyte size, indicating that there was no size bias due to the number of cells measured (Fig. S2).

Data analysis

Respiration was successfully measured from adipose tissues of 14 individuals (nine females, five males) after data from two males, both with the early maturation *vgll3* genotype, were omitted due to abnormal noise in the data. Leak CI was not determined for three individuals due to abnormal fluxes. Cryosections for adipocyte size measurements were obtained from 14 individuals (seven of each sex, after two females were omitted from the analysis due to low section quality). The males whose respiration data were excluded were included in adipocyte size measurements. For functional coherence, and to avoid biases in the female data due to different maturation status, we excluded data from the one female that displayed more advanced maturation than all others, because salmon consume the energy stored in adipose tissue during maturation (22). Given that all the remaining females in this study were immature, and all males were maturing, sex effects are confounded with maturation status throughout the study. The size, genotypes and respiration data for each individual are provided in Table S2.

Oxygen fluxes were normalised to tissue mass as well as to both tissue mass and mtDNA amount. To compare the respiration data of individuals with different *vgll3* genotypes, we focussed on data from females, as we only obtained data from two early maturation (*vgll3**EE) -genotype males.

The data were analysed in the R software environment (38), and visualised using ggplot2 (39). We tested the statistical significance of feed treatment and sex effects and of genotype effects in females using non-parametric Wilcoxon rank sum tests and Spearman's rank correlations to avoid violations of linear model assumptions due to low sample sizes. In line with the exploratory nature of this study, multiple-test correction, which is also restrictively conservative at small samples sizes, was not employed.

Results

Data overview and feed treatment effects

Because samples were obtained from salmon under different feeding treatments, we first determined the effect of diet fat content on fish phenotypes. No effects of feeding treatment were detected on fish morphology (Table 2) or respiration traits (see Fig. 2b and Fig. 3-4, where feed treatments are shown with different symbols, and Table S3) except adipocytes were significantly larger in salmon reared under a high-fat diet than a low-fat diet, as expected (Table 2). Data from the two feeding treatments were combined to improve statistical power of the subsequent analyses.

Table 2. Summary of final data sets and fish phenotypes (mean ± SD) from control (C) and low fat (LF) feed treatments. All differences between treatments were non-significant, apart from adipocyte size (results shown in footnotes). Resp = mitochondrial respiration, hist = cryohistology.

Feed	Sex	n (resp)	n (hist.)	Tissue mass resp (mg)	Fish mass (g)	Fish length (cm)	Condition factor	Gonad mass (g)	Adipocyte size (µm²)	MtDNA/ gDNA
C	F	6	4	41.7	973.8 ± 521.8	40.6 ± 8.1	1.31 ± 0.09	2.1 ± 1.8	4665.1 ± 675.5	94.3 ± 39.7
	M	4	5	40.4	1065.4 ± 462.6	41.3 ± 6.2	1.45 ± 0.14	87.8 ± 23.6	3749 ± 274.9	126.0 ± 30.9
LF	F	2	2	42.6	1244.2 ± 17.3	46.4 ± 0.1	1.25 ± 0.01	5.1 ± 3.3	3143.4 ± 605.3	83.0 ± 7.6
	M	1	2	40.9	1110 ± 164.8	44.5 ± 3.6	1.27 ± 0.12	67.8 ± 21.6	2575.3 ± 787.3	133.4 ± 1.8

Wilcoxon rank sum tests:

Control vs. LF: Fish mass W=18.0, p = 0.648; Fish length W = 15.5, p = 0.433; Condition W = 35.0, p = 0.103; Gonad mass W=19.0, p = 0.744; **Adipocyte size W = 34.0, p = 0.017;** mtDNA/gDNA W = 23.0, p = 0.948

F vs. M: Fish mass W = 29, p = 0.954; Fish length W = 28, p = 1.000; Condition W = 12, p = 0.073; Adipocyte size W = 31, p = 0.175, **mtDNA/gDNA W = 10, p = 0.043**

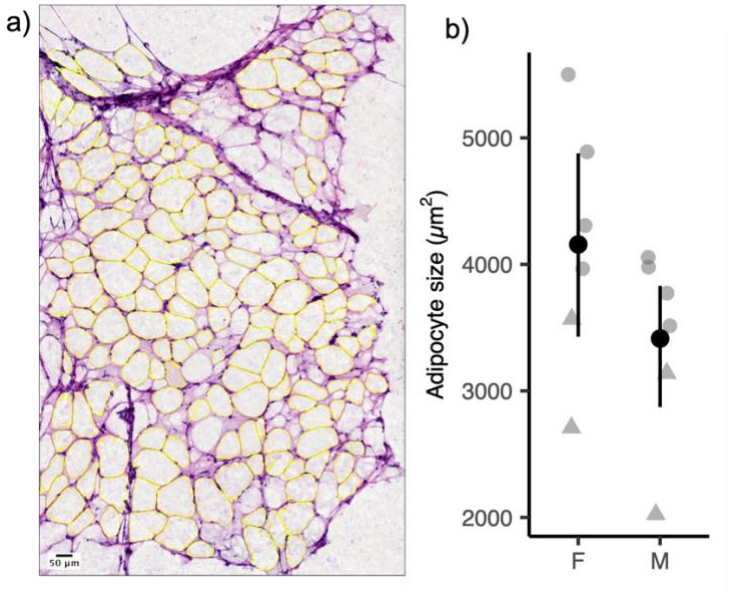

Fig. 2. Atlantic salmon adipocyte morphology. (a) Light microscope image of a representative H&E-stained cryosection of visceral adipose tissue. Measured cells highlighted in yellow (see Material & Methods section Measurement of adipocyte size). Fifty µm scale bars shown on the image, magnification 20X. (b) Mean adipocyte size (black points) ± 95 % bootstrapped confidence intervals in Atlantic salmon females and males (n_{fem} = 6, n_{male} = 7) (Wilcoxon rank sum test, Table 2, p = 0.175). Grey symbols show individual data points: circles = Control, triangles = Low fat.

Sex differences

All males had enlarged gonads indicating maturation had been initiated, but females were immature (see also Materials and methods). Males had a higher relative mtDNA amount than females (Table 2; Fig. 3a), but mitochondrial respiration did not differ between the sexes after the data were normalised either with tissue mass, or tissue mass and relative mtDNA amount (Table 3; Fig. 4a-b). This result was corroborated also by a lack of difference between the sexes in mitochondrial respiratory coefficients (Fig. S3). Interestingly, in both sexes CI-mediated respiration (NADH pathway cofactor) was substantially higher than CII-mediated respiration (succinate pathway cofactor), suggesting a generally higher preference for NADH-driven electron transfer in salmon visceral adipose tissue. There were no sex differences between any other morphological phenotypes measured nor for adipocyte size (Table 2; Fig. 2b).

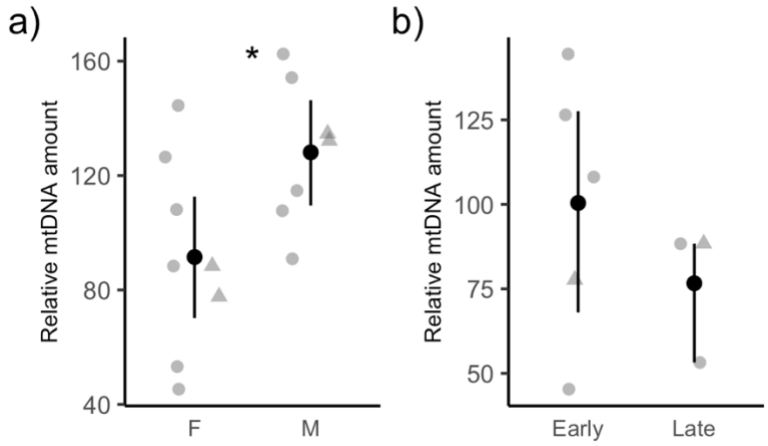

366

367 Fig. 3. Relative mtDNA amount means ± 95 % bootstrapped confidence intervals in (a) different sexes
368 and (b) only females carrying *vgll3* genotypes related to either early or late maturation. n_{fem} = 8, n_{male} =
369 7, n_{early} = 5, n_{late} = 3. Wilcoxon rank sum tests: (a) W = 10, p = 0.043 (asterisk), (b) W = 10, p = 0.551. Grey
370 points show individual data points: circles = control, triangles = low fat.
371

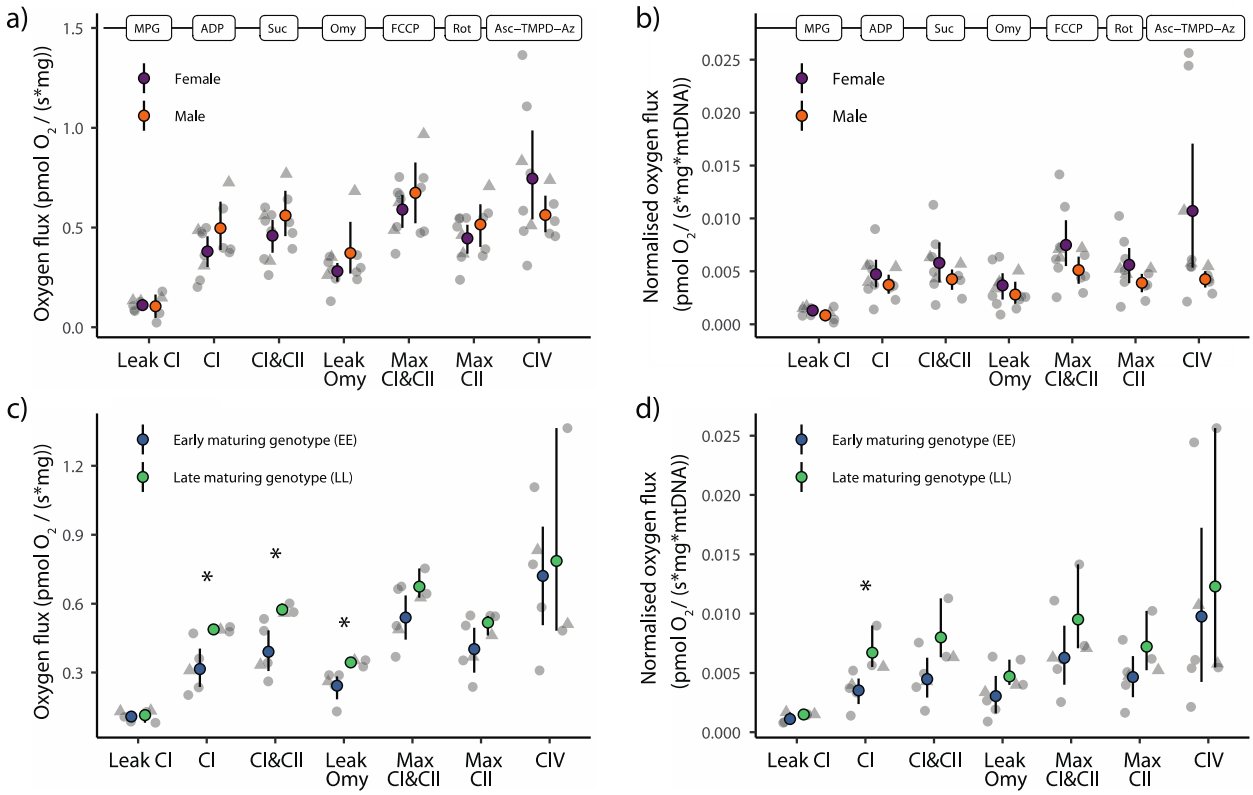

372

373 Fig. 4. Mitochondrial respiration in Atlantic salmon adipose tissue across sexes (a,b) and *vgll3* genotypes
374 (c,d). (a) and (c) mitochondrial respiration normalised to tissue mass, (b) and (d) mitochondrial
375 respiration normalised to mtDNA amount in both sexes and genotypes. n_{fem} = 8, n_{male} = 5, n_{early} = 5, n_{late} =
376 3. Added compounds for respiration measurements are shown in chronological order over the plots (see
377 Fig. 1d). Coloured points show means with bootstrapped 95% confidence intervals. Asterisks in (c) and

(d): p = 0.036 (Wilcoxon rank sum test, Table 3). Grey points show individual data points: circles = control, triangles = low fat.

Table 3. Results of Wilcoxon rank sum tests of sex- and genotype effects on mitochondrial respiration parameters normalised with tissue mass, or with tissue mass and mtDNA amount. For n see Tables 2 and 4. Significant p-values in bold.

Comparison	**Variable**	**Mass corrected**		**Mass & mtDNA corrected**	
		W	**p**	**W**	**p**
Female vs. Male	Leak CI	12	1	17	0.352
	CI	12	0.272	27	0.354
	CI&CII	14	0.421	27	0.354
	Leak Omy	15	0.51	27	0.354
	Max CI&CII	16	0.608	28	0.284
	Max CII	11	0.213	29	0.222
	CIV	27	0.341	33	0.065
Vgll3 Early vs. Late	Leak CI	4	1	3	0.7
	CI	**0**	**0.036**	**0**	**0.036**
	CI&CII	**0**	**0.036**	2	0.143
	Leak Omy	**0**	**0.036**	3	0.25
	Max CI&CII	4	0.371	2	0.143
	Max CII	4	0.371	2	0.143
	CIV	8	1	6	0.786

Vgll3 effects on mitochondrial traits

To explore the relationship between *vgll3* genotypes and mitochondrial respiration, we focussed only on female salmon (Table 4) due to the limited availability of data from males with *vgll3**EE genotype. We found that CI- and CI&CII -mediated respiration were significantly higher in individuals with the late maturation genotype compared to those with the early maturation genotype of *vgll3* (p = 0.036; Table 3; Fig. 4c). In line with the higher respiration, CI&CII -linked respiratory leak (Leak Omy) was significantly elevated in individuals with the late maturation genotype (p = 0.036; Table 3; Fig. 4c). Consequently, there was no difference between the genotypes in ATP synthesis -linked respiration rate, i.e., Leak Omy subtracted from CI&CII (mean (bootstrapped 95% C.I.): Early = 0.148 (0.0761, 0.218) and Late = 0.230 (0.207, 0.275), Wilcoxon rank sum test W = 4, p = 0.371). We then asked whether the genotype effects were mediated by the mtDNA amount –as a proxy of mitochondrial density– and found no significant differences (p = 0.551; Fig. 3b). Finally, when respiration was normalised to mtDNA amount within the same individuals, the differences were insignificant in CI&CII -mediated respiration but remained significant in CI-mediated respiration (p = 0.036; Table 3; Fig. 4d). There were no

significant effects of genotype on the other respiration traits (Table 3; Fig. 4c, d). *Vgll3* genotype effects were also mostly absent in respiration coefficients. However, the coupling capacity, P/E, of individuals carrying the late maturation genotype was marginally higher than of those carrying the early maturation genotype (p=0.071, Fig. 5).

Table 4. Summary of female salmon phenotypes (mean ± SD) across early maturation (vgll3*EE) and late maturation (vgll3*LL) genotypes. No significant differences between genotypes (see footnotes). Resp = mitochondrial respiration.

Genotype	N (resp)	Fish mass (g)	Fish length (cm)	Condition factor	Gonad mass (g)	Adipocyte size (µm)	MtDNA/gDNA
Early	5	1135.4 ± 481	43.2 ± 7.4	1.31 ± 0.1	3.7 ± 2.7	4354.1 ± 1195.2	100.4 ± 39.5
Late	3	884.8 ± 462.8	40.2 ± 8.3	1.26 ± 0.01	1.6 ± 1.1	3765.5 ± 274.4	76.7 ± 20.3

Wilcoxon rank sum tests

Early vs. Late: Fish mass W = 10, p = 0.551; Fish length W = 10, p = 0.551; Condition W = 9, p = 0.766; Gonad mass W = 12, p = 0.233; Adipocyte size W = 6, p = 0.487, mtDNA/gDNA W = 10, p = 0.551.

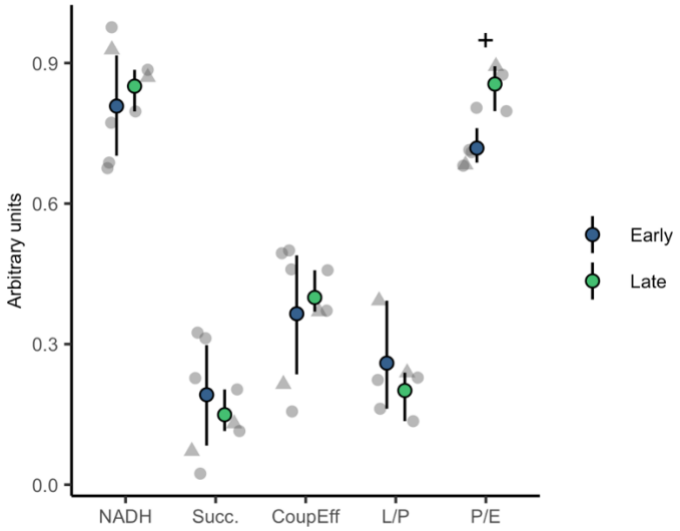

Fig 5. Respiration coefficients in female salmon with different vgll3 genotypes. The plus sign shows marginally higher coupling capacity (P/E) in the late than early maturation genotype (W = 1, p = 0.071, Wilcoxon rank sum test, nearly = 5, nlate = 3). Coloured points show means with bootstrapped 95% confidence intervals. Grey symbols show individual data points: circles = control, triangles = low fat treatment.

Correlations among fish phenotypes and mitochondrial respiration

We calculated Spearman's rank correlations between mitochondrial respiration values and fish phenotypic data, including body mass, condition factor, relative mtDNA amount and adipocyte size. There was a marginally significant negative correlation between mtDNA amount and CIV -mediated respiration (rho = -0.49, p = 0.089, Fig. S4a), but none of the other correlations were significant at alpha = 0.1 (Table S4).

Discussion

Mapping the molecular and physiological basis of life-history variation is one of the key goals of evolutionary biology. Life-history diversity within and among species is ultimately determined by energy use (17), in which adipose tissue and mitochondria functions have a central role. In this study, we provide a workflow that integrates adipose tissue mitochondrial respiration into the life-history theory framework in Atlantic salmon. Our results suggest that mitochondrial phenotypes exhibit variation associated with different backgrounds (i.e., sex/maturation, and age-at-maturity genotype). Consequently, energy generation and dissipation in the adipose tissue may have a role in the physiological determination of age-at-maturity via the *vgll3* genomic region. Below, we suggest physiological hypotheses to mechanistically link adipose tissue energetics with age-at-maturity in salmon. Our results warrant future work to test these hypotheses with larger sample sizes, across different life stages and using diverse experimental methods, and point to the significance of integrating adipose tissue mitochondrial phenotypes with life-history variation in the wild.

Overall, we verified the feasibility of measuring visceral adipose tissue mitochondrial respiration in large-sized (1 kg) Atlantic salmon. The respiration rates increased with the addition of substrates for CI and CII -mediated electron transfer, as expected. We found that visceral adipose tissue mitochondria relied more on NADH-driven CI-mediated than succinate-driven CII-mediated respiration (Fig. 4 & 5). Since NADH is generated via many different cellular processes including glycolysis, citric acid cycle and fatty acid oxidation, the activity of these cellular processes can regulate adipose tissue OXPHOS. The respiration rates were much lower than what had been earlier reported in salmonids from aerobically more active tissues, such as muscle or intestine (40, 41), but this was an expected outcome since adipose tissue is mostly composed of lipids (42). Despite the lower rate of mitochondrial respiration in adipose tissue, the L/P ratio indicated that approximately 30% of mitochondrial respiration was related to

proton leak, which is similar to the levels reported previously in fish intestine (41), but higher than that reported in gill (43), or muscle and liver (44), though it should be noted that the protocols and used in measuring Leak respiration often differ between studies. As expected, CI&CII-linked respiratory leak through entire electron transport chain (Leak Omy) was higher than CI-linked respiratory leak (Leak CI) in our study. This confirms that it is feasible to measure both coupled and uncoupled respiration in visceral fat from Atlantic salmon.

Although we showed that about 40 mg of visceral adipose tissue, measured at 12°C, provides a reasonable output as stated above, the demanding nature of the procedure due to logistic and physiological complexities should be noted. For example, adipose tissue quantity varies between individuals, and comparatively large tissue samples are required (previous studies have used, e.g., 8 mg from gill tissue (43)). We also lost data points from the lowest respiration activity, i.e., three out of 16 of our measurements were unreliable for Leak CI, which could have been avoided by using a higher amount of initial material. Even more tissue would be required to repeat the measurements for each biological replicate, which was not feasible here due to taking samples for several analyses from the same fish, though previous studies in fish have found consistent mitochondrial respiration between technical replicates (41, 43). Finally, it should be noted that since the sampled tissue can be stored only up to a few hours before the respiration measurements (unless a longer storage time is validated for this tissue (45)), coordination between the wet-lab and the field (or rearing facilities) is demanding when research is conducted on adult-sized salmonids.

Despite low power of the analyses due to low sample size, we detected significantly higher CI&CII-mediated respiration and CI&CII-linked respiratory leak, and marginally higher coupling capacity in immature female salmon with the *vgll3* late maturation genotype than in those with the early maturation genotype. These results could provide mechanistic explanations for how variation in maturation timing is linked to *vgll3* genotype, for which we postulate below two distinct but potentially complementary hypotheses.

The first hypothesis concerns resource allocation to and from the lipid deposits in adipose tissue. Maturation in Atlantic salmon is a physiological trait with a genetic threshold mediated by condition factor possibly via lipid accumulation (46). Concordantly, a previous study (20) found that *vgll3*-associated early maturation in males was mediated by a higher condition factor. In line with these previous findings, and with our results, we hypothesise that the higher mitochondrial

respiration in the adipose tissue of immature salmon with a late maturation genotype leads to reduced lipid storage, contributing to delayed maturation. Mitochondrial respiration typically increases during fasting –a state that is characterized by active catabolic metabolism. It is therefore tempting to speculate that the mitochondrial phenotype of the *vgll3* late maturation genotype could indicate active catabolic metabolism in adipose tissue. The high mitochondrial respiratory capacity could enhance the oxidation of energy substrates and subsequently reduce the size of adipose tissue depots in salmon carrying the *vgll3* late maturation genotype compared to the early maturation genotype. In line with this hypothesis, increased mitochondrial fatty acid oxidation in adipose tissue has been observed to lead to a lean phenotype in mice (47), and reduced mitochondrial respiration is related to adipocyte hypertrophy in a cell line (48). Further, a negative correlation between adiposity (body mass index, BMI) and respiration of isolated mitochondria from adipose tissue was observed in humans (49). In our study, neither genotype nor mitochondrial respiration was associated with body condition of fish (analogous to BMI). A lack of *vgll3* genotype effect on body condition in salmon was also found in the same cohort as our study fish earlier (29). However, these results do not contradict our hypothesis since body condition effects may be manifested at a different time or life-stage (20), or alternatively, was not observed due to low statistical power. For instance, salmon with the late maturation genotype could be burning their adipose tissue at a higher rate during the winter (differences in lipid utilisation have also been shown in relation to migration in juvenile salmon (50)), which would result in faster depletion of energy reserves compared to the early maturation genotype. Subsequently, the depletion of lipid reserve could delay maturation because the amount of adipose tissue in the spring is an important determinant of salmon maturation probability the following autumn (22).

The second hypothesis we propose is based on the finding that salmon with the *vgll3* late maturation genotype tended to have more actively working mitochondria and lower reserve capacity (i.e., a higher coupling capacity, P/E ratio). Electron transfer in fish with late maturation genotype was almost maximally coupled to ATP synthesis while the coupling was only up to ~70% in fish with the early maturation genotype. In the white adipose tissue of obese humans, coupling capacities of 77-83% (with an increasing trend during weight loss) have been observed (51). Thus, the adipose tissue coupling capacity in salmon with the early maturation genotype was lower compared to that in obese humans, and the higher coupling capacity in salmon with late maturation genotypes is in line with active catabolic metabolism. Because coupling capacity reflects the ability of mitochondria to adjust ATP synthesis to changes in energy demand and

supply, we also hypothesise that it could affect the resource acquisition of salmon, especially if the effect is consistent across tissues. Specifically, the lower coupling capacity in early vs. late maturation genotype could allow the fish with early maturation genotypes to increase ATP synthesis rate more during high energy demand and acute changes in environmental conditions. In contrast, salmon with the late maturation genotype with possibly higher catabolic metabolism may respond more poorly to acute increases in energy demand or stress (12), thus having less energy available to invest into survival, growth, and maturation. The mitochondria of salmon with late maturation genotype were already near-maximally coupled despite the relatively high food availability in this study (except for a 2d-period without feeding prior to sample collection). Such inherent high coupling capacity of salmon with the late maturation genotype may indicate that they could be more vulnerable to low food conditions such as during winters in freshwater (52) or in the sea (53). In line with this, a lower aerobic scope at the whole animal level –indicating lower capacity for aerobic metabolism beyond self-maintenance– in juvenile salmon with the late maturation genotype was also found by Prokkola et al. (19). Further, the lower coupling capacity of the late maturation genotype matches the distribution of salmon with contrasting age-at-maturity in the wild, where individuals maturing later spawn typically in larger rivers that are likely more environmentally stable. Further studies are required to test these hypotheses linking adipose tissue mitochondrial function and mitochondrial coupling to whole animal performance in the wild and in conditions of low food availability and fasting.

The molecular pathways that could link *vgll3* to mitochondrial respiration are not well known. In humans and mice, *vgll3* is a cofactor binding to TEA domain -containing (TEAD) transcription factors that regulates tissue differentiation pathways, such as adipogenesis and myogenesis, as well as pathways that regulate development and remodelling of tissue composition and organ and cell size, such as hippo signalling pathway (25, 54, 55). In Atlantic salmon, the widespread expression of *vgll3* is correlated with factors in the Hippo pathway (i.e. YAP, and TEAD) (56) suggesting a functional analogy in salmon with mammals. Intriguingly, the same pathways also control mitochondrial biogenesis and function (57-59), further supporting that *vgll3* genetic variation might affect mitochondrial functional variation.

We also detected sex and/or maturation effect on mtDNA amount, where (mature) males had a higher mtDNA amount (relative to gDNA) in adipose tissue than (immature) females – although there were no sex differences in mitochondrial respiration. Differences in adipose tissue

processes may emerge between mature and immature individuals, because salmon consume a large part of their adipose tissue to support the high energy demand of maturation (22, 60). A previous study also suggests that sex-specific maturation schedules could be mediated by non-visceral lipid storage, e.g., in muscle (21). Hence, future studies that partition sex and maturation status effects across tissue types would be valuable to assess the role mitochondrial variation in relation to these two phenotypes.

Conclusions

Adipose tissue is central to maturation as well as energy homeostasis but very little is known about how these two processes could be genetically interlinked. Our proof of principle study showed the feasibility of studying adipose tissue cellular respiration in salmon and yielded insightful results from which we generated informed hypotheses for future research. To further integrate adipose tissue metabolism into a life-history evolution framework, measurements of mitochondrial respiration in salmon with different *vgll3* genotypes could be combined with analyses of lipogenesis and lipolysis (i.e., lipid synthesis and release, respectively) for example using gene expression, and lipid quantification with histochemistry. Moreover, mitochondrial respiration measurements could be combined with measurements of reactive oxygen species and the effectiveness of ATP synthesis (ATP/O) (7, 61). Ultimately, to generalise the role of mitochondrial respiration and of coupling capacity in life-history evolution, studies would need to address life-stage specific genetic effects, and measurements should be extended to non-adipose tissues. Given the common physiological roles and functions of visceral white adipose tissue in salmon and humans (28), a better understanding of these functions in salmon may also facilitate its use as a new model species for obesity research. Conversely, our study provides an example of how a more advanced understanding of metabolic disorders and obesity can be harnessed to address questions relevant for ecology and evolution.

Acknowledgements

We thank Petra Liljeström, Mikko Immonen, Paul Bangura, and numerous interns for help in fish rearing at Lammi Biological Station, the Tissue Preparation and Histochemistry Unit Meilahti, University of Helsinki, for the cryosectioning and staining, and Antti Isomäki for advice on cell size measurements. Histological Imaging was supported by HiLIFE and the Faculty of Medicine, University of Helsinki, and Biocenter Finland. The study was funded by the Academy of Finland

(1328860 and 1325964 for T. A, 335443, 314383, 272376 and the Profi6 336449 funding for E.P., and 307593, 302873, 327255, and 342851 for C.R.P.), by the European Research Council under the European Articles Union's Horizon 2020 research and innovation program (grant no. 742312), and the University of Helsinki.

Online Supplemental material

Table S1. Pdf file. Primer details.

Table S2. Xlsx file. The data obtained in this study.

Appendix S1. Pdf file. Supplemental Methods, Figures, and Tables S3-S4.

Appendix S2. Txt file. A macro for adipocyte size quantification in ImageJ.

Data availability

The final data from this study is available in Table S1. The data, R codes for analyses and figures, and the images of adipose tissue sections are available in Zenodo (https://doi.org/10.5281/zenodo.6899961).

References

1. Ottaviani E, Malagoli D, Franceschi C. The evolution of the adipose tissue: A neglected enigma. General and Comparative Endocrinology. 2011;174(1):1-4.

2. Mohamed-Ali V, Pinkney JH, Coppack SW. Adipose tissue as an endocrine and paracrine organ. International Journal of Obesity. 1998;22(12):1145-58.

3. Boudina S, Graham TE. Mitochondrial function/dysfunction in white adipose tissue. Experimental Physiology. 2014;99(9):1168-78.

4. De Pauw A, Tejerina S, Raes M, Keijer J, Arnould T. Mitochondrial (Dys)function in Adipocyte (De)differentiation and Systemic Metabolic Alterations. American Journal of Pathology. 2009;175(3):927-39.

5. Martin ASG, Obin MS. Obesity and the role of adipose tissue in inflammation and metabolism. American Journal of Clinical Nutrition. 2006;83(2):461S-5S.

6. Heinonen S, Jokinen R, Rissanen A, Pietilainen KH. White adipose tissue mitochondrial metabolism in health and in obesity. Obesity Reviews. 2020;21(2).

7. Salin K, Villasevil EM, Anderson GJ, Selman C, Chinopoulos C, Metcalfe NB. The RCR and ATP/O Indices Can Give Contradictory Messages about Mitochondrial Efficiency. Integrative and Comparative Biology. 2018;58(3):486-94.

8. Kadenbach B. Intrinsic and extrinsic uncoupling of oxidative phosphorylation. Biochimica Et Biophysica Acta-Bioenergetics. 2003;1604(2):77-94.

9. Brand MD. The efficiency and plasticity of mitochondrial energy transduction. Biochemical Society Transactions. 2005;33:897-904.

10. Koch RE, Buchanan KL, Casagrande S, Crino O, Dowling DK, Hill GE, et al. Integrating Mitochondrial Aerobic Metabolism into Ecology and Evolution. Trends in Ecology & Evolution. 2021;36(4):321-32.

11. Hood WR, Austad SN, Bize P, Jimenez AG, Montooth KL, Schulte PM, et al. The Mitochondrial Contribution to Animal Performance, Adaptation, and Life-History Variation INTRODUCTION. Integrative and Comparative Biology. 2018;58(3):480-5.

12. Sokolova I. Mitochondrial Adaptations to Variable Environments and Their Role in Animals' Stress Tolerance. Integrative and Comparative Biology. 2018;58(3):519-31.

13. Chacko BK, Kramer PA, Ravi S, Benavides GA, Mitchell T, Dranka BP, et al. The Bioenergetic Health Index: a new concept in mitochondrial translational research. Clinical Science. 2014;127(5-6):367-73.

14. Dennery PA. Oxidative stress in development: Nature or nurture? Free Radical Biology and Medicine. 2010;49(7):1147-51.

15. Mobley KB, Aykanat T, Czorlich Y, House A, Kurko J, Miettinen A, et al. Maturation in Atlantic salmon (Salmo salar, Salmonidae): a synthesis of ecological, genetic, and molecular processes. Reviews in Fish Biology and Fisheries. 2021.

16. Jokinen R, Pirnes-Karhu S, Pietilainen KH, Pirinen E. Adipose tissue NAD(+)-homeostasis, sirtuins and poly(ADP-ribose) polymerases - important players in mitochondrial metabolism and metabolic health. Redox Biology. 2017;12:246-63.

17. Lailvaux SP, Husak JF. The life-history of whole-organism performance. Quarterly Review of Biology. 2014;89(4):285-318.

18. Fleming IA. Pattern and variability in the breeding system of Atlantic salmon (Salmo salar), with comparisons to other salmonids. Canadian Journal of Fisheries and Aquatic Sciences. 1998;55:59-76.

19. Prokkola JM, Asheim ER, Morozov S, Bangura P, Erkinaro J, Ruokolainen A, et al. Genetic coupling of life-history and aerobic performance in Atlantic salmon. Proceedings of the Royal Society B-Biological Sciences. 2022;289(1967).

20. Debes PV, Piavchenko N, Ruokolainen A, Ovaskainen O, Moustakas-Verho JE, Parre N, et al. Polygenic and major-locus contributions to sexual maturation timing in Atlantic salmon. Molecular Ecology. 2021.

21. House AH, Debes PV, Kurko J, Erkinaro J, Kakela R, Primmer CR. Sex-specific lipid profiles in the muscle of Atlantic salmon juveniles. Comparative Biochemistry and Physiology D-Genomics & Proteomics. 2021;38.

22. Rowe DK, Thorpe JE, Shanks AM. Role of fat stores in the maturation of male Atlantic salmon (*Salmo salar*) parr. Canadian Journal of Fisheries and Aquatic Sciences. 1991;48(3):405-13.

23. Barson NJ, Aykanat T, Hindar K, Baranski M, Bolstad GH, Fiske P, et al. Sex-dependent dominance at a single locus maintains variation in age at maturity in salmon. Nature. 2015;528(7582):405-8.

24. Sinclair-Waters M, Odegard J, Korsvoll SA, Moen T, Lien S, Primmer CR, et al. Beyond large-effect loci: large-scale GWAS reveals a mixed large-effect and polygenic architecture for age at maturity of Atlantic salmon. Genetics Selection Evolution. 2020;52(1).

25. Halperin DS, Pan C, Lusis AJ, Tontonoz P. Vestigial-like 3 is an inhibitor of adipocyte differentiation. Journal of Lipid Research. 2013;54(2):473-81.

26. Cousminer DL, Berry DJ, Timpson NJ, Ang W, Thiering E, Byrne EM, et al. Genome-wide association and longitudinal analyses reveal genetic loci linking pubertal height growth, pubertal timing and childhood adiposity. Human Molecular Genetics. 2013;22(13):2735-47.

27. Elks CE, Perry JRB, Sulem P, Chasman DI, Franceschini N, He CY, et al. Thirty new loci for age at menarche identified by a meta-analysis of genome-wide association studies. Nature Genetics. 2010;42(12):1077-U73.

28. Salmeron C. Adipogenesis in fish. Journal of Experimental Biology. 2018;221.

29. Åsheim ER, Debes PV, House A, Niemelä PT, Siren JP, Erkinaro J, et al. Strong effects of temperature, population and age-at-maturity genotype on maturation probability for Atlantic salmon in a common garden setting. bioRxiv. 2022:2022.07.22.501167.

30. Canto C, Garcia-Roves PM. High-Resolution Respirometry for Mitochondrial Characterization of Ex Vivo Mouse Tissues. Current protocols in mouse biology. 2015;5(2):135-53.

31. Djafarzadeh S, Jakob SM. High-resolution Respirometry to Assess Mitochondrial Function in Permeabilized and Intact Cells. Jove-Journal of Visualized Experiments. 2017(120).

32. Robin ED, Wong R. Mitochondrial-DNA molecules and virtual number of mitochondria per cell in mammalian cells. Journal of Cellular Physiology. 1988;136(3):507-13.

33. Guo W, Jiang L, Bhasin S, Khan SM, Swerdlow RH. DNA extraction procedures meaningfully influence qPCR-based mtDNA copy number determination. Mitochondrion. 2009;9(4):261-5.

34. Ye J, Coulouris G, Zaretskaya I, Cutcutache I, Rozen S, Madden TL. Primer-BLAST: A tool to design target-specific primers for polymerase chain reaction. Bmc Bioinformatics. 2012;13.

35. Pfaffl MW. A new mathematical model for relative quantification in real-time RT-PCR. Nucleic Acids Research. 2001;29(9).

36. Ruijter JM, Ramakers C, Hoogaars WMH, Karlen Y, Bakker O, van den Hoff MJB, et al. Amplification efficiency: linking baseline and bias in the analysis of quantitative PCR data. Nucleic Acids Research. 2009;37(6).

37. Bankhead P, Loughrey MB, Fernandez JA, Dombrowski Y, McArt DG, Dunne PD, et al. QuPath: Open source software for digital pathology image analysis. Scientific Reports. 2017;7.

38. R Core Team. R: A language and environment for statistical computing. R Foundation for Statistical Computing, Vienna, Austria; 2019.

39. Wickham H. ggplot2: Elegant Graphics for Data Analysis. Ggplot2: Elegant Graphics for Data Analysis. 2009:1-212.

40. Salin K, Auer SK, Rudolf AM, Anderson GJ, Selman C, Metcalfe NB. Variation in Metabolic Rate among Individuals Is Related to Tissue-Specific Differences in Mitochondrial Leak Respiration. Physiological and Biochemical Zoology. 2016;89(6):511-23.

41. Brijs J, Sandblom E, Sundh H, Grans A, Hinchcliffe J, Ekstrom A, et al. Increased mitochondrial coupling and anaerobic capacity minimizes aerobic costs of trout in the sea. Scientific Reports. 2017;7.

42. Nanton DA, Vegusdal A, Rora AMB, Ruyter B, Baeverfjord G, Torstensen BE. Muscle lipid storage pattern, composition, and adipocyte distribution in different parts of Atlantic salmon (Salmo salar) fed fish oil and vegetable oil. Aquaculture. 2007;265(1-4):230-43.

43. Dawson NJ, Millet C, Selman C, Metcalfe NB. Measurement of mitochondrial respiration in permeabilized fish gills. The Journal of experimental biology. 2020.

44. Salin K, Auer SK, Anderson GJ, Selman C, Metcalfe NB. Inadequate food intake at high temperatures is related to depressed mitochondrial respiratory capacity. Journal of Experimental Biology. 2016;219(9):1356-62.

45. Rees BB, Reemeyer JE, Irving BA. Interindividual variation in maximum aerobic metabolism varies with gill morphology and myocardial bioenergetics in Gulf killifish. Journal of Experimental Biology. 2022;225(12).

46. Thorpe JE. Maturation responses of salmonids to changing developmental opportunities. Marine Ecology Progress Series. 2007;335:285-8.

47. Flachs P, Rossmeisl M, Kuda O, Kopecky J. Stimulation of mitochondrial oxidative capacity in white fat independent of UCP1: A key to lean phenotype. Biochimica Et Biophysica Acta-Molecular and Cell Biology of Lipids. 2013;1831(5):986-1003.

48. Baldini F, Fabbri R, Eberhagen C, Voci A, Portincasa P, Zischka H, et al. Adipocyte hypertrophy parallels alterations of mitochondrial status in a cell model for adipose tissue dysfunction in obesity. Life Sciences. 2021;265.

49. Fischer B, Schoettl T, Schempp C, Fromme T, Hauner H, Klingenspor M, et al. Inverse relationship between body mass index and mitochondrial oxidative phosphorylation capacity in human subcutaneous adipocytes. American Journal of Physiology-Endocrinology and Metabolism. 2015;309(4):E380-E7.

50. Morgan IJ, McCarthy ID, Metcalfe NB. The influence of life-history strategy on lipid metabolism in overwintering juvenile Atlantic salmon. Journal of Fish Biology. 2002;60(3):674-86.

51. Hansen M, Lund MT, Gregers E, Kraunsoe R, Van Hall G, Helge JW, et al. Adipose tissue mitochondrial respiration and lipolysis before and after a weight loss by diet and RYGB. Obesity. 2015;23(10):2022-9.

52. Mogensen S, Post JR. Energy allocation strategy modifies growth-survival trade-offs in juvenile fish across ecological and environmental gradients. Oecologia. 2012;168(4):923-33.

53. Czorlich Y, Aykanat T, Erkinaro J, Orell P, Primmer CR. Rapid evolution in salmon life history induced by direct and indirect effects of fishing. Science. 2022;376(6591):420-+.

54. Figeac N, Mohamed AD, Sun C, Schoenfelder M, Matallanas D, Garcia-Munoz A, et al. VGLL3 operates via TEAD1, TEAD3 and TEAD4 to influence myogenesis in skeletal muscle. Journal of Cell Science. 2019;132(13).

55. Hori N, Okada K, Takakura Y, Takano H, Yamaguchi N, Yamaguchi N. Vestigial-like family member 3 (VGLL3), a cofactor for TEAD transcription factors, promotes cancer cell proliferation by activating the Hippo pathway. Journal of Biological Chemistry. 2020;295(26):8798-807.

56. Kurko J, Debes PV, House AH, Aykanat T, Erkinaro J, Primmer CR. Transcription Profiles of Age-at-Maturity-Associated Genes Suggest Cell Fate Commitment Regulation as a Key Factor in the Atlantic Salmon Maturation Process. G3-Genes Genomes Genetics. 2020;10(1):235-46.

57. Mammoto A, Muyleart M, Kadlec A, Gutterman D, Mammoto T. YAP1-TEAD1 signaling controls angiogenesis and mitochondrial biogenesis through PGC1 alpha. Microvascular Research. 2018;119:73-83.

58. Huang S, Wang X, Wu X, Yu J, Li J, Huang X, et al. Yap regulates mitochondrial structural remodeling during myoblast differentiation. American Journal of Physiology-Cell Physiology. 2018;315(4):C474-C84.

59. Liu R, Jagannathan R, Sun L, Li F, Yang P, Lee J, et al. Tead1 is essential for mitochondrial function in cardiomyocytes. American Journal of Physiology-Heart and Circulatory Physiology. 2020;319(1):H89-H99.

60. Jonsson N, Jonsson B, Hansen LP. Energetic cost of spawning in male and female Atlantic salmon (*Salmo salar* L). Journal of Fish Biology. 1991;39(5):739-44.

61. Salin K, Villasevil EM, Anderson GJ, Lamarre SG, Melanson CA, McCarthy I, et al. Differences in mitochondrial efficiency explain individual variation in growth performance. Proceedings of the Royal Society Biological Sciences Series B. 2019;286(1909):1-8.